A Study on Friction Materials for Reducing Brake Squeal by Nanotechnology

Kenji Abe*
Masaaki Nishiwaki*
Yukihiro Shiomi*
Yasuo Fujioka**
Hiromichi Yanagihara***
Igor Stankovic***

Abstract
Brake squeal can be attributed to dynamic instability of vibration systems and friction force variation. Recent developments have seen the practical application of methods for reducing brake squeal by improving the dynamic stability of brake design. These methods use FEM calculations based on dynamic instability theory, but have not been studied in depth because of the difficulty of reducing friction force variation. This article describes a study in which molecular dynamics was applied to the design of friction materials. Simulation results for the friction force of resins were validated experimentally, and the study showed that improving the design of friction materials is an effective way of reducing brake squeal.

Keywords: *brakes, friction materials, simulation, squeal, nanotechnology, friction force variation*

1. Introduction

In general terms, noise such as high-pitch brake squeal occurs more frequently when the friction coefficient μ is high.[1][2] This has been shown to be the result of dynamic instability of the vibration systems that made up the brakes, suspension, and knuckles.[2][3]

Methods for reducing brake squeal by improving the dynamic stability of structures have already been put into practice. These methods use FEM calculations based on models of contact states between components such as the calipers, disc rotors, and knuckles.[4]

However, since it is not easy to design dynamic stability for every natural frequency mode of the vibration systems, there is a crucial need for research into reducing brake squeal by reducing friction force variation. Despite this, virtually no cases of such research have been published.

The research described in this article discusses a method of reducing friction force variation not covered by dynamic stability analysis, and the validation of this method by experiment.

2. Effect of Brake Friction Surfaces on Friction Coefficient μ

Brake pads are a composite material comprising several tens of different raw materials in which friction and abrasion modifiers are added to a base material with phenol resin as a binder.

When the brakes are run in, material components from the brake pads adhere to the friction surfaces of the gray cast iron disc rotors, forming a friction film. This friction film has a large effect on the friction coefficient μ.[5]

Since this surface friction film contains phenol resin, it should be possible to reduce friction force variation by improving the polymer resins such as the phenol resin blended into the brake pad.

To verify the brake squeal reduction effect in this research, the base material of the brake pad was designed based on a commercially available type to be more susceptible to squeal. A prototype friction material containing a replacement for phenol resin was then produced for binding the base material, and tests were performed to verify that it reduced brake squeal without reducing the friction coefficient μ.

3. Reduction of Friction Force Variation of Polymer Resin

3.1 Modeling of polymer

First, as shown in **Fig. 1**, a model was created of a single bead was created using monomer masses connected with springs.[6] Multiple examples of this model were then strung together to create a polymer bead model.

* Chassis Development Div.
** Vehicle Engineering Development Div.
*** Toyota Motor Europe NV/SA R&D

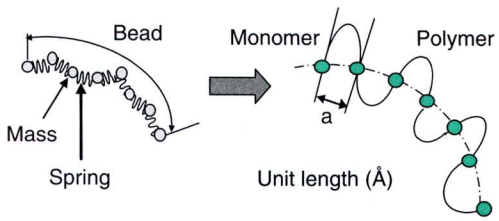

Fig. 1 Monomer and Polymer Models[7]

The flexibility of the polymer can be expressed based on its molecular structure (monomer type, co-polymer proportion, stereoregularity, and so on) and the persistence length lp. The persistence length lp, in other words, the length at which the polymer chain can maintain linearity, is calculated according to Equation 1. If its value is large, then the polymer has a high bending rigidity and is less likely to become tangled when friction is applied. The lp value is determined by the bond structure and, when the length of the polymer is less than the lp, it has little effect on macro behavior such as the friction coefficient μ. It should also be noted that lp=0 equals a theoretical rigidity of zero.

$$lp = a\,(C_\infty + l) / 2 \qquad (1)$$

where,

a: bond length between bead masses[6] (unit length shown in **Fig. 1**)

C_∞: characteristic ratio[6]

In molecular level measurement, each characteristic value is often expressed as a non-dimensional number to prevent digit overflow. In addition, to improve the degree of freedom of display in the calculations, a previously proposed design method was applied.[6] The standard lp value and the like were expressed in a finitely extendable nonlinear elastic (FENE) spring model to enable the characteristic values of the polymer to be compared. The nondimensional parameters can be converted into dimensional parameters using Equation 2, and the details of this are described in reference material (6).

$$Q_{ref.} = m^{\alpha+\beta/2}\, r_0^{\beta+r}\, \varepsilon^{-\gamma/2} \qquad (2)$$

3.2 Equation of motion

The behavior of each monomer can be calculated by the equation of motion shown in Equation 3. The dominant external force of the potential function acts depending on the distance r between each monomer. This external force changes over time from the initial value $F_{int.}$ to the maximum value $F_{max.}$ before relaxing into a final value. The rate of this change is determined by the aging time coefficient D and the relaxation time coefficient τ. In this way, it is possible to calculate the time-based changes in friction force using a model that also considers viscoelasticity.

$$M\ddot{x} = k_s(v_s t - x) - \eta(\dot{x})\dot{x}A - F_{max.} - (F_{int.} - F_{max.})(1 - e^{-\phi(t)/\tau})$$
$$\dot{\phi} = 1 - \dot{x}\phi D \qquad (3)$$

where,

M: monomer mass

k_s: spring stiffness

v_s: shear rate

η : damping factor

$F_{int.}$: initial value of external force

D: aging time coefficient

x: displacement

t: time

A: area

$F_{max.}$: maximum value of external force

τ: relaxation time coefficient

Fig. 2 shows outline views describing how friction force variation increases when the real contact area changes dramatically. When the friction surface displaces faster than the relaxation time, the friction force variation becomes large. This characteristic is governed by the aging time coefficient D and the relaxation time coefficient τ. Accordingly, if time-based changes in friction force due to aging are suppressed, then the variation will decrease (right side of **Fig. 2**)

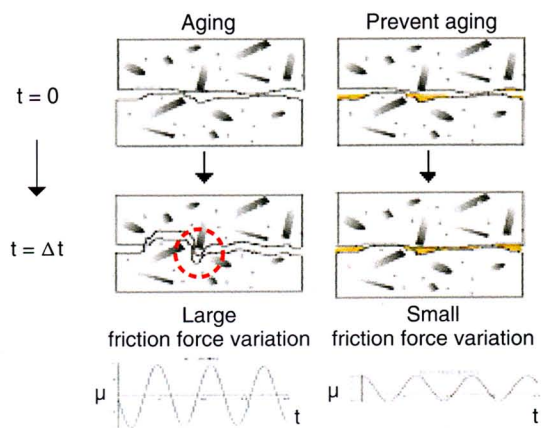

Fig. 2 Friction Force Variation of Polymer

As shown in **Fig. 2**, a polymer structure was considered in which the stress partially does not increase in accordance with the dramatic changes in the real contact area when the polymer undergoes shear deformation. As a result, it was found that friction force variation can be reduced by a polymer structure with a straight chain molecular structure.[8]

In specific terms, instead of a three-dimensional net-like molecular structured polymer such as phenol resin, a two-dimensional straight chain molecular structured polymer such as polyamideimide (PAI) should be capable of reducing friction force variation.

3.3 Considerations for stabilizing friction coefficient μ

This section describes a general mechanism for generating friction. From both macroscopic and microscopic standpoints of friction, the friction coefficient μ can be expressed in general as the sum of three types of friction: (1) the friction generated by the polymer arrangement and geometrical shape as shown in Equation 4, (2) the friction determined by the ratio between the shear viscosity and polymer diffusion rate as shown in Equation 5, and (3) the friction determined by the length of the polymer chains and the monomer bond rigidity (the ease of polymer entanglement and its capacity to absorb shear energy) as shown in Equation 6.

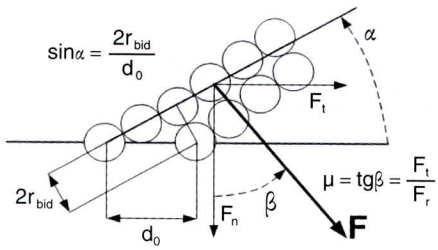

$2r_{bid}$: bead diameter
$d_{surf} = d_0$: distance between beads
α : angle between polymer and friction surface
β : angle of direction of force acting on polymer

Fig. 3 Polymer Model Based on Molecular Dynamics

Equation 4 shows that this type of friction is determined by the geometrical factors shown in **Fig. 3** (such as angle α and the like) and the unit volume of polymer chains (i.e., the density of the polymer). Thus, it can be derived from the balance of forces.

$$\mu_1 = \frac{2\frac{r_{bid}}{d_{surf}} + A}{\sqrt{1-\left(2\frac{r_{bid}}{d_{surf}}\right)^2}} \quad (4)$$

where,

A : constant

In addition, with respect to the phenomenon whereby the viscous resistance increases when the velocity of the viscous fluid is close to zero, μ_2 can be determined by Equation 5.

$$\mu_2 = \left(1+\frac{6k_BTDL}{v}\right) \quad (5)$$

where,

v: shear fluid velocity
T: temperature in Kelvin
D: diffusion constant
k_B: Boltzman's constant
L: polymer layer thickness

Additionally, Equation 6 shows how the number of beads in the polymer chain N_{bits} and the FENE spring rigidity constants (k_{FENE} in Equation 5) govern the friction coefficient μ. The basic length of polytetrafluoroethylene (PTFE) can be calculated as follows: $l_{ref.}=[(Tm/Tm^*)\times k_B/\text{yield stress}]^{1/3}$. If a PTFE yield stress of 100 MPa and the characteristic values are substituted into the equation, then $l_{ref.}$=4.9 Å is obtained. Therefore, the number of the FENE polymer for persistence length (N_{bits}-lp) becomes 19.3 Å/4.9 Å=3.9.

$$\mu_3 = \frac{1}{1-\frac{C_N}{N_{bids}}-\frac{C_K}{k_{FENE}}} \quad (6)$$

where,

C_N: constant
C_K: constant
N_{bids}: lp/lp*
1p*: persistence length in FENE model
k_{FENE}: FENE spring rigidity constants

In this way, the friction coefficient μ was obtained by calculation to enable how variation in μ can be suppressed. **Fig. 4** shows that if the number of the FENE polymer for persistence length (N_{bits}-lp) is small, then variation in the density of the polymer chains (N_{chain}) facilitates variation in μ. In contrast, if the number of the FENE polymer for persistence length (N_{bits}-lp) is large, then variation in the density of the polymer chains (N_{chain}) hampers variation in μ. Therefore, a large μ with little variation can be created by increasing both the number of the FENE polymer for persistence length (N_{bits}-lp) and the density of the polymer chains (N_{chain}).

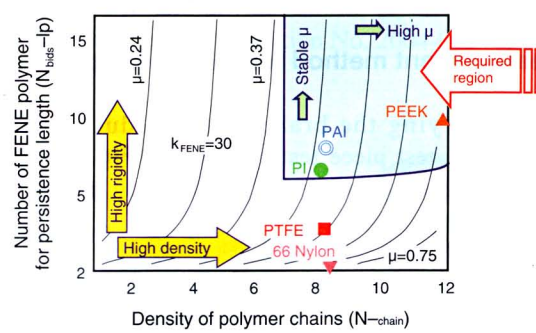

Fig. 4 Effect of Number of FENE Polymer for Persistence Length and Density of Polymer Chains on Friction Properties

Fig. 5 shows that if the FENE spring rigidity constants (k_{FENE}) are low, then variation in the polymer density facilitates variation in μ. In contrast, if the FENE spring rigidity constants (k_{FENE}) are high, then variation in μ is low. Therefore, it should be possible to maintain μ at a high level with little variation by increasing both the FENE spring rigidity constants (k_{FENE}) and the density of the polymer chains (N_{chain}), even if the

temperature of the friction surface rises and the FENE spring rigidity constants (k_{FENE}) change.

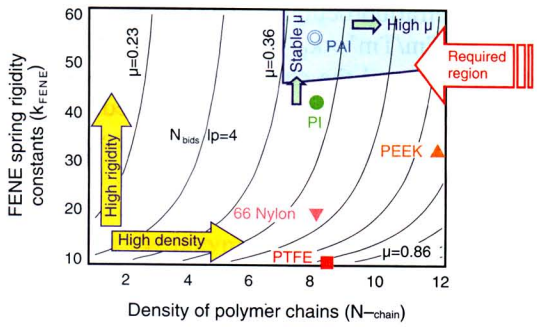

Fig. 5 Effect of FENE Spring Rigidity Constants and Density of Polymer Chains on Friction Properties

Thus, a resin in which the density of the polymer chains (N_{chain}) per unit area is 6 or higher, the number of the FENE polymer for persistence length (N_{bits}-lp) is 6 or higher, and the FENE spring rigidity constants (k_{FENE}) are 50 or higher should be capable of achieving a high friction coefficient μ with low variation.

4. Verification of Brake Squeal Reduction by Experiment

Since conventional phenol resin has a three-dimensional net-like molecular structure, it is more susceptible to friction coefficient μ variation than a resin with a straight chain molecular structure. Therefore, replacing the conventional resin with a straight chain molecular structured resin like PAI should deter the generation of brake squeal even when μ is high.

4.1 Measurement method for friction properties

Before verifying the brake squeal reduction effect by experiment, the test piece tester shown in **Fig. 6** was used to measure the friction coefficient μ by detecting the friction force with a strain gauge.

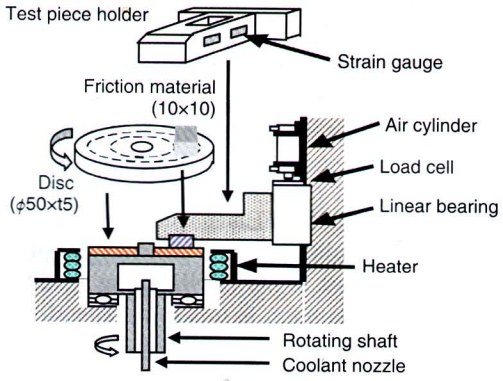

Fig. 6 Tester for Measuring Test Piece Friction Properties[9]

4.2 Friction properties of polymer resin test pieces

Figs. 4 and **5** predict that PAI has the most stable μ and that, although polyetheretherketone (PEEK) and polyimides (PI) have stable μ at normal temperatures, the variation in μ of these materials will be greater than PAI when the temperature increases.

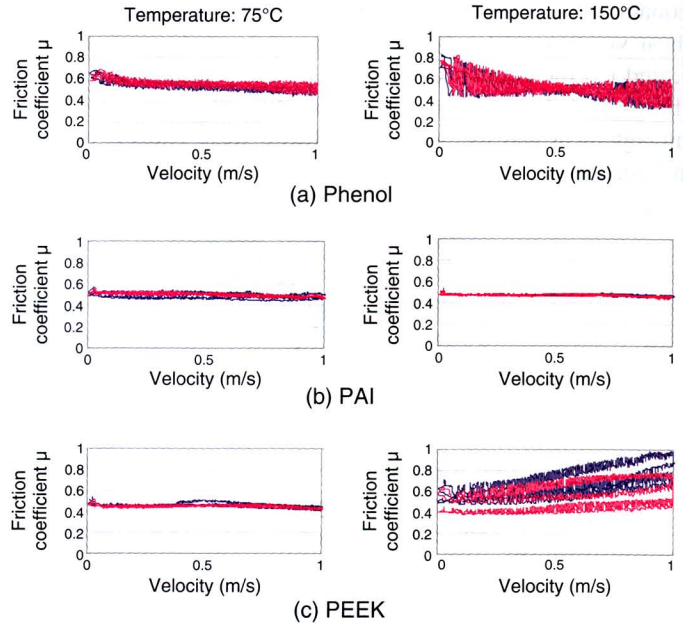

Fig. 7 Friction Properties of Polymer (Test Pieces)

Fig. 7 shows the results of the verification tests. Even at a temperature of 75°C, the phenol resin has a large variation in μ. This variation becomes even larger at 150°C. It was verified that the negative slope of the load with respect to sliding velocity v (dμ/dv) for phenol was larger than that for PAI. Moreover, although PEEK has low variation in μ at 75°C, the variation increases rapidly at 150°C. These results correspond closely with the calculated values for μ, validating the appropriateness of the predictions.

4.3 Verification of effect using improved friction material

Friction experiments using parts formed from phenol resin and polymer PAI that satisfied the requirements derived from **Figs. 4** and **5** were able to verify the improvement in μ stability. The next step was to produce a prototype brake pad and verify the calculation results that it should be capable of reducing brake squeal without reducing μ.

Break squeal was examined using a front disc brake of a compact passenger car attached through a knuckle to a dynamometer.

Running in (1,000 times) was performed on the new pad under urban driving conditions to stabilize the state of the friction surface, after which the ease that brake squeal could be generated was examined. Brake squeal was obtained using a sound level

meter, analyzed by FFT, and the frequency peaks were plotted on a graph. The brake friction coefficient μ was measured at the same time during approximately 500 braking operations.

Fig. 8 shows the results of the experiment. The figure indicates that the occurrence of brake squeal was halved by adopting a brake pad using PAI instead of phenol resin. Furthermore, as shown in **Fig. 9**, the squeal noise was reduced by approximately 20 dB with the brake friction coefficient μ at the same level of 0.42.

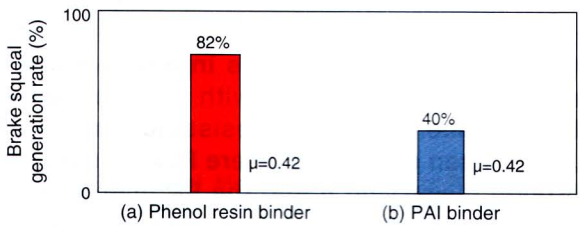

Fig. 8 State of Brake Squeal Generation (Dynamometer)

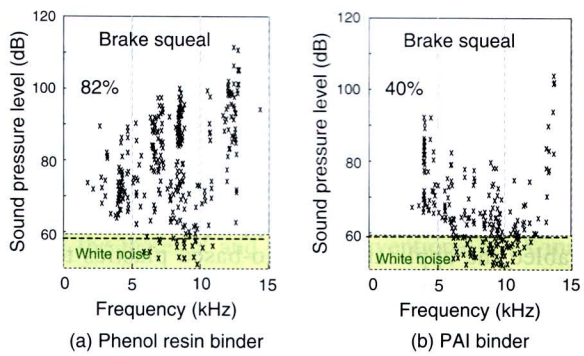

Fig. 9 Brake Squeal Test Results (Dynamometer)

5. Conclusions

(1) The molecular structure of a polymer capable of maintaining a high friction coefficient while reducing variation was determined by calculation. A prototype brake pad was then produced in which the conventional resin was replaced with PAI. PAI was selected as it has a molecular structure close to that determined by the calculation. It was subsequently verified by experiment that this pad was capable of decreasing brake squeal while reducing the variation in friction coefficient without lowering the coefficient itself.

(2) The required properties of a polymer capable of maintaining the friction coefficient at a high level with little variation were identified. It was found that the number of the FENE polymer for persistence length (N_{bits}-lp), which indicates the bending rigidity of the polymer, should be 6 or higher, the unit area density of the polymer chains (N_{-chain}) should be 6 or higher, and the FENE spring rigidity constants (k_{FENE}) should be 50 or higher.

(3) A brake pad produced using a resin binder that satisfies these requirements was found to be capable of improving brake squeal without reducing the effectiveness of the brakes.

Finally, the authors would like to extend their gratitude to Mr. Ryoji Goto, Mr. Yoshio Shimura, and Mr. Yuji Nagasawa of Toyota Central R & D Labs., Inc., and Mr. Tatsuhisa Kubota, Mr. Hiroyuki Fujikawa, and Mr. Tomoyuki Wakamatsu of Advics Co., Ltd.

References

(1) M. Erikson, Jacobsen. "Friction Behavior and Squeal Generation of Disc Brakes at Low Speeds." *Proceedings of the Institution of Mechanical Engineers Part D: Journal of Automobile Engineering* (2001) pp. 1245-1256.

(2) N Millner. "An Analysis of Disc Brake Squeal." *SAE Paper* No.780332 (1978).

(3) M. Nishiwaki. "Study on Brake Noise: 5th Report, Generalized Theory of Brake Noise." *Transactions of the Japan Society of Mechanical Engineers C* Vol. 56 No. 527 (1990) pp. 1782-1788.

(4) G. Liles. "Analysis of Disc Brake Squeal Using Finite Element Methods," *SAE Paper* No. 891150 (1989).

(5) N. Odani, Kobayashi, Kakihara. "Discussion on Disc Brake Pad μ" (in Japanese). *Proceedings of the Society of Automotive Engineers of Japan* No. 97-98 9839399 (1998) pp. 5-8.

(6) H. Yanagihara, Kroeger. *Design Method and System for Polymer Material*. Japanese Patent Application No. 2005-163662.

(7) M. Kroeger. "Simple Models for Complex Non Equilibrium Fluids." *Physics Reports* (2004) pp. 453-551.

(8) M. Nishiwaki, Fujioka, Abe, Yanagihara. *Design Method for Sliding Materials with Low Noise and Vibration* (in Japanese). Japanese Patent Application No. 2008-263956.

(9) Y. Nagasawa, Yoshida, Hashimoto, Nishiwaki. *Friction Tester*. Japanese Patent Publication No. 2004-012172.

Authors


K. ABE


M. NISHIWAKI


Y. SHIOMI


Y. FUJIOKA


H. YANAGIHARA

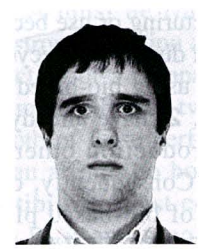
I. STANKOVIC